Relationship between Meat Structure, Water Mobility, and Distribution: A Low-Field Nuclear Magnetic Resonance Study

HANNE CHRISTINE BERTRAM,*,† PETER PATRICK PURSLOW,‡,§ AND
HENRIK JØRGEN ANDERSEN†

Department of Animal Product Quality, Danish Institute of Agricultural Sciences, Research Centre
Foulum, P.O. Box 50, DK-8830 Tjele, Denmark, and Department of Dairy & Food Science,
The Royal Veterinary and Agricultural University, Rolighedsvej 30, DK-1958 Frederiksberg, Denmark

Nuclear magnetic resonance (NMR) measurements were carried out on pork longissimus muscle, which pre rigor had been manipulated to various muscle lengths, to investigate the relationship between the microstructure of meat and the NMR T_2 relaxation. Distributed exponential analysis of the NMR T_2 relaxation data revealed the existence of three distinct water populations: T_{2b}, T_{21}, and T_{22}. A high, significant correlation was found between the T_{21} time constant and the sarcomere length ($r = 0.84$) and calculated ration of myofilament lattice volume in the I-band and A-band regions, respectively ($r = 0.84$), considering sigmoid relationships. The result implies that the T_{21} time constant mainly is determined by the structure of the myofilament lattice and so strongly supports a previously proposed theory that the T_{21} population corresponds to water located within a highly organized myofibrillar protein matrix including actin and myosin filament structures. A high correlation was also found between the T_{22} population and the water-holding capacity (WHC) ($r = 0.76$), which suggests that the WHC is mainly determined by the amount of loosely bound extramyofibrillar water. However, the correlation between NMR T_2 parameters and WHC was further increased ($r = 0.84$) by including the T_{21} time constant in the correlation analysis. This implies that the formation of drip loss is an ongoing process involving the transfer of water from myofibrils to the extracellular space and is affected by structural features at several levels of organization within the muscle tissue. This study demonstrates the advantages of NMR T_2 relaxation as an effective technique for obtaining further understanding of the relationship between the microstructure of meat, its WHC, water mobility, and water distribution.

KEYWORDS: Water-holding capacity; contraction; sarcomere length; pork; NMR T_2 relaxation; myofibrillar lattice

INTRODUCTION

Water-holding capacity (WHC) is a very important quality trait in pork (*1*, *2*) and has a high economic significance. Large variations in WHC can occur, and much attention has been given to the mechanisms that control it and the means to reliably measure it (*3*). Renou et al. (*4*) were first to show that low-field (LF) nuclear magnetic resonance (NMR) relaxation measurements correlated with certain meat characteristics such as pH, cooking loss, and protein denaturation. Later, Tornberg et al. (*5*) demonstrated the potential use of spin−spin relaxation times (T_2) in LF NMR studies to differentiate pork with considerable variation in WHC. This interesting study inspired further work, and it has been subsequently demonstrated that the technique can successfully discriminate pork with a quite narrow variation in WHC in highly optimized production systems (*6*). This finding was further enhanced by recent data demonstrating that the potential drip loss from meat can be related directly almost to a single water population detected by NMR T_2 relaxation (*7*).

The establishment of a high correlation between NMR T_2 relaxation and WHC has stimulated further interest in understanding the relation of individual T_2 parameters to the distribution of water and thereby WHC in meat. Manipulation of meat structure by either physical or chemical means in a recent NMR T_2 relaxation study has made it possible to define relations between the three distinct water populations detected by NMR T_2 relaxation in meat and the physical/anatomical structures within the meat (*8*). Thus, the T_{2b} relaxation time (centered on times in the order of 1−10 ms) corresponds to water bound to proteins (*9*), the T_{21} relaxation time (centered on times in the order of 40−60 ms) relates to water trapped within the myofibrils, and the T_{22} relaxation time (centered on times in the range of 150−400 ms) corresponds to water outside the myofibrillar lattice and also outside the muscle cell. However,

* To whom correspondence should be addressed. Tel: +45 89 99 15 06. Fax: +45 89 99 15 64. E-mail: HanneC.Bertram@agrsci.dk.
† Research Centre Foulum.
‡ The Royal Veterinary and Agricultural University.
§ Current address: Department of Biological Sciences, University of Stirling, Stirling FK9 4LA, U.K.

Meat Structure and Water Distribution

J. Agric. Food Chem., Vol. 50, No. 4, 2002 **825**

further detailed studies are needed to confirm the proposed relationship between the individual NMR T_2 relaxation parameters and the distribution of water within the microstructural features of meat. The aim of the present study was to investigate these concepts by testing the possible relationships between the myofilament lattice spacing and the NMR T_2 relaxation parameters measured in pork samples with a wide variation in sarcomere length.

MATERIALS AND METHODS

Sampling and Sample Preparation. Porcine longissmus muscles from both sides of one commercially available animal were obtained within 1 h of slaughter at a nearby slaughterhouse. The left-hand muscle was divided longitudinally into two parts (contracted (C) and normal (N)). Part C was immediately cut into 20 subsamples (approximately 5 cm long and 2 cm × 2 cm in cross-sectional area), wrapped individually in polyethylene bags, and placed in ice water in order to induce cold shortening. After the muscles were immersed in ice water for approximately 2 h, they were transferred to storage at 4 °C until 24 h post mortem. Part N of the muscle was kept in a polyethylene bag at 15 °C for 6 h to allow rigor development and then stored at 4 °C until 24 h post mortem when it was sampled and cut into 20 subsamples (approximately 5 cm along the fiber direction and 2 cm × 2 cm in cross-sectional area). The second muscle was also immediately cut into 16 subsamples approximately 8 cm along the fiber direction and 3 cm × 3 cm in cross-sectional area. (The wider cross section was chosen to allow for narrowing of the samples upon stretching.) From these 16 subsamples, 4 samples were each stretched to approximately 125, 150, 175, and 200% of rest length, respectively. (Half of the samples for each degree of stretching were stretched out by clamps attached to a hand-driven extensional screw thread. The other half were lengthened by tight wrapping of the cross section of the samples with polyethylene film to obtain the desired lengthening of the prerigor meat.) All stretched (S) samples were kept for 6 h at 15 °C to allow rigor mortis to develop and then stored at 4 °C until 24 h post mortem. At 24 h post mortem, the S subsamples were divided into two parts, resulting in a total of 36 S subsamples.

Preparation of Myofibrils. Myofibrils from porcine *M. longissimus* were isolated according to the procedure given by Olson et al. (*10*) for the determination of the myofibrillar fragmentation index. A buffer containing 100 mM KCl, 20 mM K_2HPO_4 (pH 7), 1 mM EGTA, 1 mM $MgCl_2$, and 1 mM NaN_3 was used for washing. After three washings, the myofibrils were suspended in a buffer containing 25 mM citric acid (pH 5.2, $I = 0.16$ M) and kept overnight before centrifugation at first 15 min at 2000g and thereafter at 2 × 30 min at 12 000g.

Determination of Drip Loss. At 24 h post mortem, all of the subsamples ($n = 76$) were cut into equal-sized rectangles (approximately 4 cm along the fiber direction and 2 cm × 2 cm in cross-sectional area), placed in a net with the fiber direction aligned vertically, and then hung until 144 h post mortem within individual polyethylene bags to eliminate significant evaporative losses. During this period, the samples were taken out and weighed at 24, 48, and 120 h, and drip loss was calculated as the percentage weight loss.

Determination of Sarcomere Length. At 24 h post mortem, a small sample (approximately 100 mg) was taken from each of the 76 subsamples, fixed in 4% paraformaldehyde in 100 mM mesylate buffer containing 0.9% NaCl, pH 5.6, and stored at 4 °C until required. Sarcomere length was then determined by examination of thick longitudinal cryosections under a Leica DMIRB microscope using Image Pro Plus software (Image House A/S, Denmark) to determine the Z-disk spacing as the mean from 9 subsampled areas of the microscope image.

NMR Measurements. The relaxation measurements were performed on a Maran Benchtop Pulsed NMR Analyzer (Resonance Instruments, Witney, U.K.) with a magnetic field strength of 0.47 T, with a corresponding resonance frequency for protons of 23.2 MHz.

The NMR instrument was equipped with an 18 mm temperature variable probe. At 144 h post mortem, T_2 was measured using the Carr−Purcell−Meiboom−Gill sequence (*11, 12*). The T_2 measurements were performed with a τ-value (time between 90 and 180° pulse) of 150 μs, and the lengths of the pulses were 7.8 and 15.6 μs for the 90 and 180° pulse, respectively. Data from 4096 echoes were acquired as 16 scan repetitions. The repetition time between two succeeding scans was 2 s, which allowed the longitudinal relaxation to return to equilibrium ($T_1 = 0.8$ s). All relaxation measurements were performed at 25 °C.

Distributed exponential fitting analysis was performed on the T_2 relaxation data using the RI Win-DXP program (software release version 1.2.3) released from Resonance Instruments Ltd., U.K. The RI Win-DXP program performs distributed exponential curve fitting. A continuous distribution of exponentials for a CPMG experiment may be defined by eq 1

$$g_i = \int_0^\infty A(T) \times e^{-ti/T} \, dT \tag{1}$$

where g_i is the intensity of the decay at time ti and $A(T)$ is the amplitude of the component with transverse relaxation time T. The RI Win-DXP program solves this equation by minimizing the function

$$(g_i - \int_{x=1}^m f_x \, e^{-ti/Tx})^2 + \lambda \sum_{x=1}^m f_x^2 \tag{2}$$

where $f_x = \int_{T_x}^{T_{x+1}} A(T) \, dT \cdot \lambda\sum_{x=1}^m f_x^2$ is a linear combination of functions added to the equation in order to perform a zero-order regularization as described by Press et al. (*13*). The data were pruned from 4096 to 256 points using linear pruning, which on synthetic data was found to give stabile solutions. This analysis resulted in a plot (see **Figure 2**) of relaxation amplitude for individual relaxation processes vs relaxation time. From such analyses, time constants for each process were calculated from the peak position, and the area under each peak (corresponding to the proportion of water molecules exhibiting that relaxation time) was determined by cumulative integration using an in-house program written in Matlab (The Mathworks Inc., Natick, MA).

Statistical Analysis. Analysis of variance was carried out using the GLM procedure from the Statistical Analysis System (*14*). The statistical models used included the fixed effects of sample treatment (C, S, and N). In addition, multiple linear regression (MLR) was carried out using the MLR procedure.

RESULTS

Drip loss was observed to vary with muscle sarcomere length. The drip loss at 120 h post mortem for all subsamples is shown plotted against measured sarcomere length in **Figure 1a**. Despite considerable variability in measured drip, it is readily apparent that drip loss was lower for samples with long sarcomere lengths and higher for the C samples. **Figure 1b** shows the mean drip loss for C, N, and S groups at 24, 48, and 120 h. A progressive increase in drip loss was seen for all treatments.

Figure 2 shows typical examples of results obtained upon distributed exponential fitting on T_2 relaxation data from C, S, and N meat samples. Three components, hereafter referred to as T_{2b}, T_{21}, and T_{22}, were detected in all meat samples: a minor component between 1 and 10 ms (T_{2b}), a major component between 40 and 60 ms (T_{21}), and finally a third component between 150 and 400 ms (T_{22}).

In **Table 1** the meantime constants and corresponding proportions of the water molecule population for each relaxation component are given for the C, S, and N meat samples. The time constants differed significantly between C and S samples and N and S samples, with exception of the T_{2b} time constant. In contrast, no significant difference was found between the C and the N samples. Moreover, the T_{21} and T_{22} water populations differed significantly between C, S, and N samples, respectively, while the T_{2b} populations did not differ between samples.
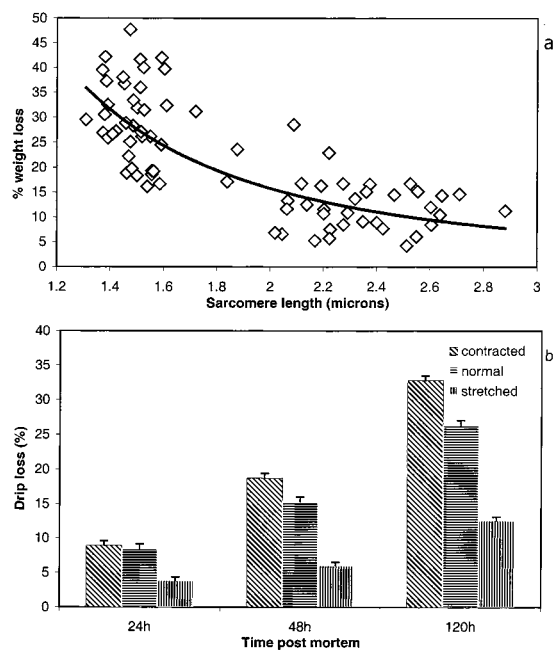
Figure 1. Drip loss vs muscle length. (**a**) Percent weight loss as drip after 120 h post mortem vs sarcomere length for all samples. (**b**) Mean drip loss determined at 24, 48, and 120 h post mortem for C ($n = 20$), S ($n = 16$), and N ($n = 20$) meat samples, respectively. Bars indicate standard errors.
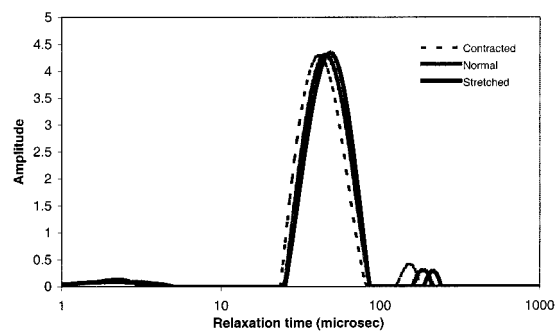

Figure 2. Representative distribution of T_2 relaxation times for C, N, and S meat measured 144 h post mortem. T_2 data were performed with a τ-value (time between 90 and 180° pulse) of 150 μs. Measurements were performed at 25 °C, and data were acquired from 4096 echoes as 16 scan repetitions with a repetition time of 2 s between two succeeding scans.

Table 2 shows the calculated correlation coefficients between drip loss (120 h post mortem) and NMR characteristics. Strongly significant correlations were found between the drip loss and the T_{21} and T_{22} time constants and corresponding populations; the highest correlation was found between the T_{22} population and the WHC.

In **Figure 3**, the relationship between the sarcomere length and the peak value of the T_{21} time constant is plotted for all samples. The two variables were found to be sigmoidal correlated (sarcomere length = $3.86/(1 + e^{(-T_{21}-44.10/5.19)})$), with a correlation coefficient of $r = 0.84$.

Figure 4 shows the distributed exponential fitting of NMR T_2 relaxation data from isolated myofibrils. A relaxation pattern similar to that obtained in the meat samples was observed. In agreement with the T_2 relaxation data from the meat samples, three components were detected; a minor component ($\approx 3-4\%$) at approximately $1-2$ ms (T_{2b}), a major component ($\approx 94\%$) at approximately 45 ms (T_{21}), and finally a third component ($\approx 2\%$) at approximately $300-400$ ms (T_{22}).

Table 1. Relaxation Time Constants and Corresponding Populations Measured 144 h Post Mortem for the Three Treatments[a]

| | treatment | | | | | | significance level | | |
| | C | | N | | S | | | | |
	$\bar{X}$	SE	$\bar{X}$	SE	$\bar{X}$	SE	C vs N	C vs S	N vs S
	Time Constants (ms)								
T_{2b}	1.97	0.04	2.03	0.04	2.11	0.03		**	
T_{21}	45.22	0.30	45.14	0.30	46.66	0.34		***	***
T_{22}	170.6	4.8	177.6	4.8	209.1	5.3		***	***
	Populations (%)								
T_{2b}	3.19	0.09	3.10	0.09	3.25	0.07			
T_{21}	93.67	0.15	94.48	0.15	95.52	0.11	***	***	***
T_{22}	3.10	0.12	2.35	0.12	1.17	0.13	***	***	***

[a] Least-squares means and standard errors (SE) are given. Different letters in rows indicate significant differences between treatments.

Table 2. MLR Correlation Coefficients and Levels of Significance for the Correlations between the Time Constants T_{21}, T_{22}, and the Corresponding Populations and Drip Determined ($n = 75$)

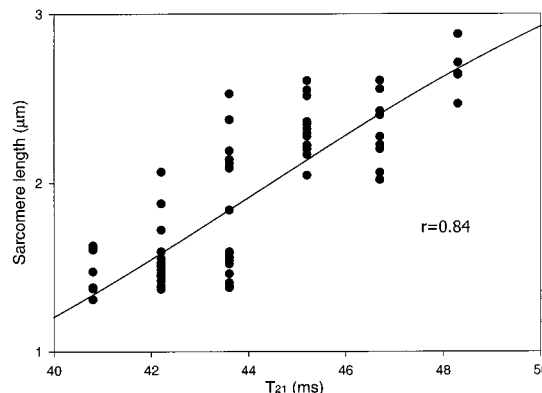| T_2 parameter(s) in the statistical model	drip loss (144 h)	T_2 parameter(s) in the statistical model	drip loss (144 h)
T_{2b} (ms)	−0.21	T_{2b} area	−0.12
T_{21} (ms)	−0.61***	T_{21} area	−0.67***
T_{22} (ms)	−0.74***	T_{22} area	0.76***

Figure 3. Relationship between sarcomere length and top point of the T_{21} time constant ($n = 75$). Data were fitted to the function sarcomere length = $3.86/(1 + e^{-(T_{21}-44.10/5.19)})$.

DISCUSSION

The main constituent of meat is water, which makes up approximately 76 wt % of fresh meat. The second major constituent is protein, which makes up approximately $20-22$ wt % of the meat. The amount of water directly associated with protein ("bound" water) is only about 0.5 g water per 1 g protein (*3*). The major part of the water in the meat must therefore be held physically within subcellular (myofibrillar) structures, and it is reasonable to postulate that differences in muscle structure will affect the water distribution and thereby the WHC of the meat. The present study demonstrates a significant correlation between the final sarcomere length and the drip loss from the meat. This is in agreement with a previous study by Honikel et al. (*15*), which concentrated on the relationship in cold-shortened vs resting muscle, but extends the observations also to longer sarcomere lengths. These findings suggest that WHC is indeed affected by the structural features of the meat that change with sarcomere shortening.

It has been suggested (*15*) that expulsion of the fluid located between the thick and the thin filaments of the myofibrillar
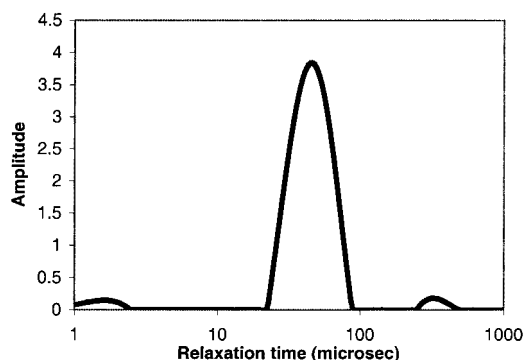
Meat Structure and Water Distribution

J. Agric. Food Chem., Vol. 50, No. 4, 2002   **827**

Figure 4. Distribution of T_2 relaxation times for purified myofibrils. T_2 data were performed with a τ-value (time between 90 and 180° pulse) of 150 μs. Measurements were performed at 25 °C, and data were acquired from 4096 echoes as 16 scan repetitions with a repetition time of 2 s between two succeeding scans.

system should explain the correlation between sarcomere shortening and WHC. However, this remains to be investigated.

The multiexponential T_2 relaxation in inhomogeneous, compartmentalized systems has previously been discussed extensively (16−20). Despite certain discrepancies, it is generally agreed that the relaxation must depend on spatial factors, as surfaces such as membranes and insoluble protein filaments are expected to act as relaxation sinks for the water molecules (20). Whether or not a surface actually will act as a relaxation sink for a certain water molecule depends on the distance from the molecule to the surface. If the time taken for a water molecule to diffuse to the surface is longer than its relaxation time, the water molecule will not experience the surface as a relaxation sink. In contrast, if the distance to the surface is such that the time for the water molecule to diffuse to the surface is shorter than the relaxation time, the water molecule's relaxation will be affected by the surface acting as a relaxation sink due to exchange processes between the protons on the surface and the water (17). In association with these ideas, Brownstein and Tarr (17) suggested that the relaxation of water protons depends on the relaxation strength and the probability of the water protons meeting the surface, the latter expressed as the surface-to-volume ratio of the structure, which confines the water protons. Accordingly, the T_2 relaxation time can be expressed as eq 3 (17):

$$(1/T_2) = \mu(S/V) \tag{3}$$

where μ is the relaxation sink strength, S is the surface area, and V is the volume. This approach has later been used by Hills et al. (21, 22) and others (23−26) to analyze T_2 relaxation data quantitatively.

The present study was carried out to enlighten possible relationships between LF NMR T_2 relaxation parameters and sarcomere length. In accordance with earlier studies (7, 8), continuous distributed exponential analysis of the T_2 relaxation revealed the presence of three distinct water populations (T_{2b}, T_{21}, T_{22}) in all meat samples. The anatomical nature of the muscle reveals that the length of the inherent sarcomeres varies within highly defined boundaries with defined upper and lower limits. Consequently, a sigmoid relationship between sarcomere length and parameters reflecting it must be expected. A highly significant, positive correlation ($r = 0.84$) was found between the intermediate time constant (T_{21}) and the sarcomere length of the muscle samples when fitting to a sigmoid function

(sarcomere length $= a/(1 + e^{-(T_{21}-x_0/b)})$) (**Figure 3**). This indicates that structural features associated with changes in sarcomere length directly affect the mobility of water characterized by the T_{21} component. A recent study on frog muscles also reported a similar relationship between the structure of the myofibrillar water and the degree of contraction (27). To further substantiate this relationship, it becomes reasonable to reveal (i) which water population is the T_{21} component reflecting, i.e., where is the water physically/anatomically present within the fiber and (ii) which structural changes within the muscle fiber can be positively correlated to an increase in the T_{21} time constant.

The majority (93−96%; **Table 1**) of the population of water molecules shows relaxation behavior characterized by the intermediate relaxation time constant (T_{21}). It has previously been suggested that the intermediate time constant (T_{21}) reflects water located within highly organized myofibrillar protein structures, e.g., water in tertiary and/or quaternary protein structures and spatial domains with high myofibrillar protein densities including actin and myosin filament structures (8). Under the assumption that the structures are similar to cylinders the S/V ratio will be given by eq 4

$$(S/V) = (2\pi r l/\pi r^2 l) = (2/r) \tag{4}$$

Accordingly, assuming that the water is located between the thin and the thick filaments, which are separated by a distance of approximately 40 nm (28) results in an S/V ratio of approximately $2/r = 5 \times 10^7$ m^{-1}. A T_{21} value of approximately 45 ms as found in the present study results in a corresponding relaxation sink strength of $\mu = 0.44$ nm/ms (eq 3). Unfortunately, no numbers for relaxation sink strength in biological matrixes are directly available in the literature. However, the found value is comparable with numbers obtained in porous silica glass, silica spheres, and treated coals, which span the area of 0.1−0.2, 0.1, and 0.03−0.9 nm/ms, respectively (24−26). Accordingly, from a quantitative point of view, it seems reasonable that the T_{21} component can be ascribed to water located within highly organized myofibrillar protein structures, e.g., water in tertiary and/or quaternary protein structures and spatial domains with high myofibrillar protein densities including actin and myosin filament structures. Moreover, T_{21} times in the order of 45 ms were also seen in the preparation of purified myofibrils, which fundamentally demonstrates that the principal relaxation sink delimiting the structural domain characterized by T_{21} is to be found at the level of the myofibrillar structure.

In the exploitation of which structural changes within the muscle fiber that correspond to an increase in the T_{21} time constant (ii), it is noteworthy that prerigor muscle stretch and contract at a constant volume. This reveals that an increase in sarcomere length gives rise to (i) a decrease in the diameter of the fiber, (ii) a decrease in the diameter of the myofibrils contained in each fiber, and (iii) a decrease in the lateral spacing between thick and thin filaments within the sarcomere (28, 29).

All of these structural changes upon an increase in sarcomere length result in a reduction in the S/V ratio (eq 4), and a decrease in the T_2 time constant representing water within the concerned structure should accordingly be expected (eq 3). Interestingly, the opposite was found in the present study, why none of the above-mentioned structural changes (i, ii, and iii) upon an increase in sarcomere length seem to explain the present findings.

Changes in sarcomere length (s) of porcine longissimus muscle have empirically been related to X-ray diffraction
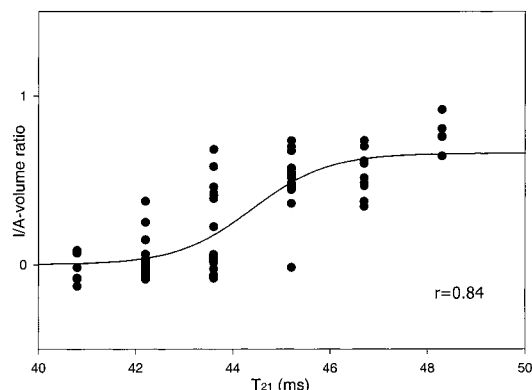
Figure 5. Relationship between calculated ratio of myofilament lattice spacing in the I-region and the A-band region and top point of the T_{21} time constant ($n = 75$). Data were fitted to the function sarcomere length $= 0.66/(1 + e^{-(T_{21}-44.39/0.78)})$.

measurements of the distance (d) between thick filaments according to eq 5 (*28, 29*)

$$d = -2.8998s + 38.161 \qquad (5)$$

To a first approximation, d also corresponds to the center-to-center distance between thin filaments in mammalian muscle where the thin filaments occur in the centroid position between the hexagonal array of thick filaments. The sliding filament hypothesis proposed by Huxley (*30−32*) predicts that the I-band will shorten during contraction, while the A-band of the sarcomere will keep the original length, independent of the degree of contraction. Accordingly, an increase in sarcomere length results in an increase in the proportion of the sarcomere occupied by the I-band (which contains thin filaments only, as opposed to the A-band, which contains both thick and thin filaments). The I-band region is the area of the sarcomere that has the least protein density, and accordingly, it could be expected that the rate of relaxation of water within the I-band would be slower than the rate of relaxation of water within the A-band area, which has a higher protein density. In other words, the reason for the observed increase in the T_{21} time constant with increasing sarcomere length could be that a higher proportion of water is located within the I-band as opposed to within the A-band. As the A-band has been found to have a length of approximately 1.5 μm (*31*), the myofilament lattice volume in the I-band region can be calculated using eq 6

$$\text{volume}_{\text{I−band}} = (s - 1.5) \cdot d^2 \cdot 3^{1/2}/4 \qquad (6)$$

where s is again the sarcomere length and d is the thick filament spacing. This shows that changes in sarcomere length directly affect the myofilament lattice volume in the I-band region. Using the same approach, the myofilament lattice volume in the A-band region can likewise be calculated using eq 7

$$\text{volume}_{\text{A−band}} = 1.5 \cdot d^2 \cdot 3^{1/2}/4 \qquad (7)$$

Accordingly, the ratio between the volume of the I-band and the A-band is given by eq 8

$$\frac{\text{volume}_{\text{I−band}}}{\text{volume}_{\text{A−band}}} = \frac{s - 1.5}{1.5} = \frac{s}{1.5} - 1 \qquad (8)$$

In **Figure 5** the relationship between the ratio of myofilament lattice space in the I-region and the A-region (I/A volume ratio) and the peak value of the T_{21} time constant is shown. Fitting

the two variables to a sigmoid function gives a correlation coefficient of 0.84. This must be predicted as the I-band and A-band volume data are direct derivatives of the sarcomere length, which was found to display a sigmoid relationship with the T_{21} time constant with a correlation of $r = 0.84$. Some of the measured mean sarcomere lengths had a length below 1.5 μm from which eq 4 predicts a negative I-band volume and thereby a negative I/A volume ratio, and this of course is unrealistic. When the sarcomere length becomes shorter than the thick filament length, the I-band simply disappears because the thick filaments are directly pushed up against the Z-disks at each end of the sarcomere. However, despite this reservation, these simple calculations should principally give a meaningful reflection of relationship between the degree of contraction and the ratio of myofibrillar lattice volume in the I-band and A-band regions, respectively. Consequently, the correlation between the relaxation rate of the intermediate time constant (T_{21}) and the ratio of myofibrillar lattice volume in the I-band and A-band regions may explain the observed increase in the T_{21} time constant with increasing sarcomere length. Finally, it should be noticed that considering eq 3, it cannot with present data be ruled out that the increase in the T_{21} time constant upon increasing sarcomere length might depend on the relaxation sink strength (μ), if this parameter changes with changes in sarcomere length. This might not be trivial, as stretching might change the myofibrillar protein structures and the corresponding morphology, which then affect the surface properties and hereby the relaxation sink strength (μ). However, further intensive studies are needed to reveal this aspect.

A smaller proportion of the total relaxation signal is characterized by a longer time constant T_{22}. In agreement with a recent study (*7*), a highly significant correlation was also found here between the WHC (determined as drip loss) and the T_{22} population ($r = 0.76$). The T_{22} population can therefore be considered as potential drip loss. However, as the T_{22} water population is drained out of extracellular spaces and is lost as drip, diffusion and pH-induced lateral contraction of the myofilament lattice drives the transport of water from the highly organized myofibrillar matrix into the extramyofibrillar matrix. The rate at which this transport will occur, and thereby the rate of formation of new potential drip, must be expected to depend on how tightly the water is associated to the environment within the highly organized myofibrils. This suggests that relaxation characteristics of water in both the myofibrillar and the extramyofibrillar matrix may be jointly related to drip. Accordingly, a correlation analysis including both the T_{22} population and the T_{21} time constant was carried out. This analysis revealed a correlation coefficient of 0.84 between the T_{22} population and the T_{21} time constant and drip loss. Consequently, the mobility (extent of binding) of the water located within the highly organized myofibrillar protein matrix, together with the amount of loosely bound extramyofibrillar water, determine the formation of drip. The formation of drip from meat may be considered a continuous process, which includes the mobilization of water from the highly organized myofibrillar protein matrix into the extramyofibrillar space in addition to expelling of water from the extramyofibrillar space to the cut meat surface.

CONCLUSION

In conclusion, the present study demonstrated a strong and significant correlation between the intermediate time constant (T_{21}) from LF NMR relaxation signals from the water in meat and the sarcomere length. These findings support the hypothesis that the intermediate time constant (T_{21}) reflects water located

Meat Structure and Water Distribution

J. Agric. Food Chem., Vol. 50, No. 4, 2002 **829**

within highly organized protein structures of the myofibrils. Water in tertiary and/or quaternary protein structures and spatial domains with high myofibrillar protein densities (including actin and myosin filament structures) may be involved. However, this study focuses attention on the volume in the I-band area of myofibrils as being a domain of interest. Moreover, it demonstrates the importance of structural features within muscle tissue for water mobility and distribution and, hence, the final WHC of the meat.

ACKNOWLEDGMENT

LITERATURE CITED

(1) Trout, G. R. Techniques for Measuring Water-Binding Capacity in Muscle Foods- A Review of Methodology. *Meat Sci.* **1988**, *23*, 235–252.

(2) den Hertog-Meischke, M. J. A.; van Laack, R. J. L. M.; Smulders, F. J. M. The water-holding capacity of fresh meat. *Vet. Q.* **1997**, *19*, 175–181.

(3) Offer, G.; Knight, P. The structural basis of water-holding in meat Part 2: Drip Losses. In *Developments in Meat Science −4*; Lawrie, R., Ed.; Elsevier Applied Science: London, 1988; Chapter 4, pp 172–243.

(4) Renou, J. P.; Monin, G.; Sellier, P. Nuclear Magnetic Resonance Measurements on Pork of Various Qualities. *Meat Sci.* **1985**, *15*, 225–233.

(5) Tornberg, E.; Andersson, A.; Göransson, Å.; von Seth, G. Water and Fat Distribution in Pork in Relation to Sensory Properties. In *Pork Quality*: *Genetic and Metabolic Factors*; Puolanne, E., Demeyer, D. I., Ruusunen, M., Ellis, S., Eds.; CAB International: Wallingford, 1993; pp 239–256.

(6) Bertram, H. C.; Andersen, H. J.; Karlsson, A. H. Comparative study of low-field NMR relaxation measurements and two traditional methods in the determination of water holding capacity of pork. *Meat Sci.* **2001a**, *57*, 125–132.

(7) Bertram, H. C.; Dønstrup, S.; Karlsson, A. H.; Andersen, H. J. Continuous distribution analysis of T2 relaxation in meat − An approach in the determination of water holding capacity. *Meat Sci.* **2002b**, *60*, 279–285.

(8) Bertram, H. C.; Karlsson, A. H.; Rasmussen, M.; Dønstrup, S.; Petersen, O. D.; Andersen, H. J. The origin of multiexponential T_2 relaxation in muscle myowater *J. Agric. Food Chem.* **2001c**, *49*, 3092–3100.

(9) Belton, P.; Jackson, R. R.; Packer, K. J. Pulsed NMR studies of water in striated muscle: I. Transverse nuclear spin relaxation times and freezing effects. *Biochim. Biophys. Acta* **1972**, *286*, 16–25.

(10) Olson, D. G.; Parrish, F. C.; Stromer, M. H. J. Myofibril fragmentation and shear resistance of three bovine muscles during postmortem storage. *J. Food Sci.* **1976**, *41*, 1036–1041.

(11) Carr, H. Y.; Purcell, E. M. Effects of Diffusion on Free Precession in Nuclear Magnetic Resonance Experiments. *Am. J. Phys.* **1954**, *94*, 630–638.

(12) Meiboom, S.; Gill, D.; Huxley, H. E.; Niedergerke, R. 1958. Modified spin−echo method for measuring nuclear times: Measurement of the striations of isolated muscle fibres with interference. *Rev. Sci. Instrum.* **1958**, *29*, 688–691.

(13) Press, W. H.; Teukolsky, S. A.; Vetterling, W. T.; Flannery, B. P. Intregral Equations and Inverse Theory. *Numerical Recipes in Fortran*, 2nd ed.; Cambridge University Press: New York, 1992; Chapter 18.

(14) SAS user's guide: Statistics, version 6, 4th ed.; SAS Institute, Inc.: Cary, NC, 1991.

(15) Honikel, K. O.; Kim, C. J.; Hamm, R. Sarcomere Shortening of Prerigor Muscles and Its Influence on Drip Loss. *Meat Sci.* **1986**, *16*, 267–282.

(16) Hazlewood, C. F.; Chang, D. C.; Nichols, B. L.; Woessner, D. E. Nuclear Magnetic Resonance transverse relaxation times of water protons in skeletal muscle. *Biophys. J.* **1974**, *14*, 583–606.

(17) Brownstein, K. R.; Tarr, C. E. Importance of classical diffusion in NMR studies of water in biological cells. *Phys. Rev. A* **1979**, *19*, 2446–2453.

(18) Lillford, P. J.; Clark, A. H.; Jones, D. V. Distribution of Water in Heterogeneous Food and Model Systems. In *Water in Polymers*; Rowland, S. P., Ed.; ACS Symposium Serie*s* 127; American Chemical Society: Washington, DC, 1980; pp 177–195.

(19) Belton, P.; Ratcliffe, R. G. NMR and compartmentation in biological tissues. *Prog. NMR Spectr.* **1985**, *17*, 241–279.

(20) Hills, B. P.; Takacs, S. F.; Belton, P. S. Interpretation of Proton NMR Relaxation Time Measurements of Water in Food. *Food Chem.* **1990**, *37*, 95–111.

(21) Hills, B. P.; Snarr, J. E. M. Dynamic q-space microscopu of celluar tissue. *Mol. Phys.* **1992**, *76*, 979–994.

(22) Hills, B. P.; Belton, P. S.; Quantin, V. M. Water proton relaxation in heterogeneous systems: I. Saturated, randomly packed suspensions of impenetrable particles. *Mol. Phys.* **1993**, *78*, 893–908.

(23) Davis, S.; Packer, K. J. Pore-size distribution from NMR spin−lattice relaxation measurements of fluid-saturated porous solids. *J. Appl. Phys.* **1990**, *67*, 3163–3170.

(24) D'Orazio, F.; Tarczon, J. C.; Halperin, W. P.; Eguchi, K.: Mizusaki, T. Application of nuclear magnetic resonance pore structure analysisi to porous silica glass. *J. Appl. Phys.* **1989**, *65*, 742–751.

(25) Gallegos, D. P.; Munn, K.; Smith, D. M.; Sterner, D. L. A NMR Technique for the Analysis of Pore Structure: Application to Materials with Well-Defined Pore Structure. *J. Colloid Interface Sci.* **1989**, *119*, 127–140.

(26) Glaves, C. L.; Davis, P. J.; Gallegos, D. P.; Smith, D. M. Pore structure analysis of coals via low-field spin−lattice relaxation measurements. *Energy Fuels* **1988**, *2*, 662–668.

(27) Yamada, T. ^{1}H NMR spectroscopy of the intracellular water of resting and rigor frog skeletal muscle. In *Mechanisms of Work Production and Work Absorption in Muscle.* Sugi, H., Pollack, G. H., Eds.; Plenum Press: New York, 1988; pp 145–155.

(28) Diesbourg, L.; Swatland, H. J.; Millman, B. M. X-ray diffraction measurements of postmortem changes in the myofilament attice of pork. *J. Anim. Sci.* **1988**, *66*, 1048–1054.

(29) Schäfer, A.; Knight, P. J.; Wess, T. J.; Purslow, P. P. Influence of sarcomere length on the reduction of myofilament lattice spacing post-mortem and its implication in drip loss. *Proc. 46th Intl. Congr. Meat Sci. Technol.* (*Buenos Aires*) **2000**, 406–407.

(30) Huxley, H. E.; Hanson, J. Quantitative studies on the structure of cross-striated myofibrils. *Biochim. Biophys. Acta* **1957**, *23*, 229–249.

(31) Huxley, H. E.; Niedergerke, R. Measurement of the striations of isolated muscle fibres with interference microscope. *J. Physiol.* **1958**, *144*, 403–425.

(32) Huxley, H. E. Evidence for continuity between the central elemnets of the triads and extracellular space in frog sartorius muscle. *Nature* **1964**, *202*, 1067–1071.